

**16th International Conference on  
Harmonisation within Atmospheric Dispersion Modelling for Regulatory Purposes  
8-11 September 2014, Varna, Bulgaria**

---

**A LABORATORY INVESTIGATION OF FLOW AND TURBULENCE OVER A TWO-DIMENSIONAL URBAN CANOPY**

*Annalisa Di Bernardino<sup>1</sup>, Paolo Monti<sup>1</sup>, Giovanni Leuzzi<sup>1</sup> and Giorgio Querzoli<sup>2</sup>*

<sup>1</sup> DICEA, University of Rome “La Sapienza”, Via Eudossiana 18, Rome. Italy

<sup>2</sup> Dipartimento di Ingegneria del Territorio, Università di Cagliari. Italy

**Abstract:** A neutral boundary layer was reproduced in the laboratory to analyse the wind field in correspondence of a two-dimensional array of buildings. The study has been conducted in a water channel. The measurements were performed along a vertical plane, parallel to the streamwise velocity and perpendicular to the obstacles. The goal was to examine in detail how the aspect ratio  $AR=W/H$  influences the velocity field (here  $H$  is the building height and  $W$  the road width). In particular, an analysis of the mean velocity, turbulent kinetic energy, Reynolds stress, skewness factor, production of the turbulent kinetic energy and its rate of dissipation is conducted for  $AR$  ranging from 1 to 2. Particular attention is focused on the Reynolds stress, one of the parameters mostly affected by the aspect ratio.

**Key words:** *2-D building array, Canopy layer, Roughness sublayer, Street canyon, Water channel*

## **INTRODUCTION**

In the last decades, the interaction between urban areas and atmosphere has obtained increasing attention by the scientific community. This is due, in particular, to the rapid growth of population in large cities, that determines air pollution and human comfort degradation. One of the most important parameters used to describe urban fabric geometries is the aspect ratio  $AR=W/H$ , where  $H$  is the height of the building and  $W$  the street width. According to past studies, Oke T. (1987) summarized the nature of the flow in urban canopies in terms of  $AR$ . He defined three different kind of regimes: the skimming flow ( $AR \lesssim 1.5$ ), in which only a single vortex develops within the street canyon, the wake interference flow ( $1.5 \lesssim AR \lesssim 2.5$ ), which allows the development of two counter-rotating vortexes and the isolated obstacle regime ( $AR \gtrsim 2.5$ ), where the flow strictly resembles that observed for the isolated building case. Both 2D and 3D building arrays have been extensively investigated in the past through numerical simulations, laboratory experiments and field campaigns (see, among others, Jeong S.J. and Andrew M.J., 2002; Kastner-Klein P. and Rotach, 2004; Lien F.S. et al., 2004; Soulhac L. et al., 2008; Salizzoni P. et al., 2011). Despite the increasing research efforts of the recent years, a number of questions regarding the turbulence characteristics above and within the urban canyon still remain open. For example, the way in which the vertical structure of the roughness sublayer (RSL, i.e. the region above the canopy where the flow is influenced by the individual roughness elements) depends on  $AR$  is not well-clear. Furthermore, the validity of the canonical log-law in modeling the vertical profile of the wind speed in urban areas must be considered with circumspection (Pelliccioni et al., 2014).

The present work deals with a laboratory investigation of the neutrally-stratified boundary layer in correspondence of a two-dimensional array of buildings. A water channel was used for the experiments. The goal was to examine the turbulence characteristics in the canopy layer as well as the processes by which the flow within the canopy layer exchanges energy and momentum with the overlaying fluid layers. Two spatial configurations are mainly investigated, i.e.  $AR=1$  and 2. The former corresponds with the skimming flow regime, while the latter to the wake interference flow. Both the cases are of particular interest because they represent urban fabric configurations typical for many large cities.

## **EXPERIMENTAL SET-UP**

The experiments were performed using a close-loop water channel, located at the Hydraulics Laboratory

of the University of Rome - La Sapienza, Italy (Figure 1). The channel is 35 cm high, 25 cm wide and 740 cm long. The flume is fed by a constant head reservoir. During all the experiments, the water depth was set to  $h=16.5$  cm. The test section is located nearly 500 cm downstream of the channel inlet, where the boundary layer can be considered fully-developed. Small pebbles (averages diameter of 5 mm) were displaced over the channel bottom in order to increase the roughness of the surface and to produce the typical logarithmic vertical profiles of the streamwise velocity.

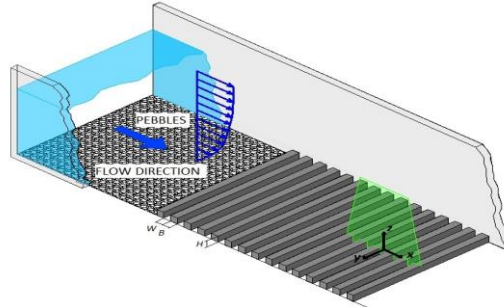


**Figure 1.** Modelled urban canopy representation. H indicates the building height while  $B=H$  is its width. W is the distance between two successive buildings

The facility consists of a hydraulic system, a High Speed-CMOS-Camera and a green laser (wavelength 532 nm). For all the experiments, the frame rate was set to 250 frames per second and each acquisition lasts 40 s. Velocity measurements were performed using the Feature Tracking (Miozzi et al., 2008) along a vertical plane parallel to the streamwise velocity and perpendicular to the canyons axis. The test area is 9.9 cm long (x-axis - streamwise direction) and 7.2 cm height (z-axis - vertical direction). A spatial, Gaussian interpolation algorithm was applied to the instantaneous velocity samples in order to obtain a two-dimensional Eulerian description of the motion on a  $99 \times 72$  regular grid along the x- and z-axis, respectively, with a spatial resolution of 0.1 cm. We define the origin ( $x=0$ ,  $z=0$ ) at the centre of the investigated area, considering x positive downstream and z upward. The Reynolds number  $Re = (U \cdot h/\nu)$  of the flow was  $\sim 44000$ , where  $U=27$  cm  $s^{-1}$  is the mean free stream velocity and  $\nu=100$  cm<sup>2</sup>  $s^{-1}$  is the kinematic viscosity of water. Each building is simulated by means of a parallelepiped rod of square section  $B=H=2$  cm and length 25 cm, the latter corresponding with the channel width (see Figure 1).

## RESULTS

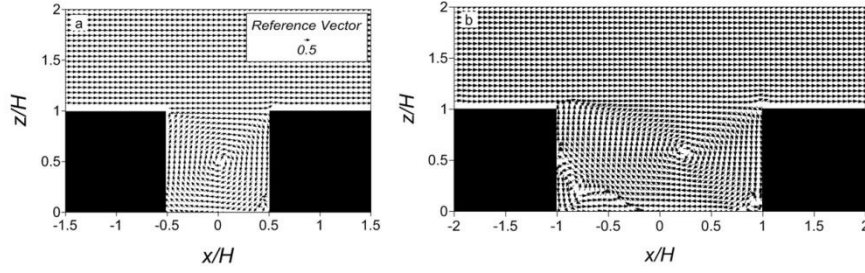
### Mean velocity

Figure 2 shows a vector representation of the mean velocity field referred to  $AR=1$  (a) and 2 (b). The streamwise velocity is directed rightward. Velocity components are expressed as  $\bar{u}/U$  and  $\bar{w}/U$ , where u and w are the streamwise and the vertical velocity components, respectively (overbar indicates time averages calculated over the time duration of the experiment). For  $AR=1$  the flow pattern conforms to the skimming flow regime, i.e. a nearly horizontal current flowing parallel to the x-direction above the canopy and a main vortex which occupies most of the canyon, characterized by smaller velocity. The vortex is slightly shifted downstream and towards the top of the canyon, while, at the bottom-right corner of the canyon, a small, counter-rotating vortex is present, in agreement with results reported in the literature (see for example LES results by Li X.X. et al., 2010). For  $AR=2$  the main vortex is significantly shifted downstream and a well-defined counter-rotating vortex forms near the leeward building.

### Vertical momentum flux and turbulent kinetic energy

Colour maps of the non-dimensional, vertical momentum flux,  $\overline{u'w'}/U^2$ , for  $AR=1$  and 2 are shown in Figure 3. As expected, the values are negative above the canyon for both the configurations, while, inside the canyon, the sign of  $\overline{u'w'}/U^2$  strongly depends on AR, i.e. it is mostly negative for  $AR=1$  and positive for  $AR=2$ . It is worthwhile discussing the behaviour of  $\overline{u'w'}/U^2$  and the mean streamwise velocity above the canopy (i.e. within the RSL) as a function of AR (see Figure 4, where,  $\langle \cdot \rangle_{x_C+R}$  denotes the spatial

averaging performed along the  $x$ -axis in the area overlaying the canyon top, C, and one rooftop, R). Two additional aspect ratios were also considered for the analysis, namely  $AR=1.5$  and  $1.75$ .



**Figure 2.** Mean velocity vectors for  $AR=1$  (a) and  $AR=2$  (b). Velocity components are normalized by  $U$

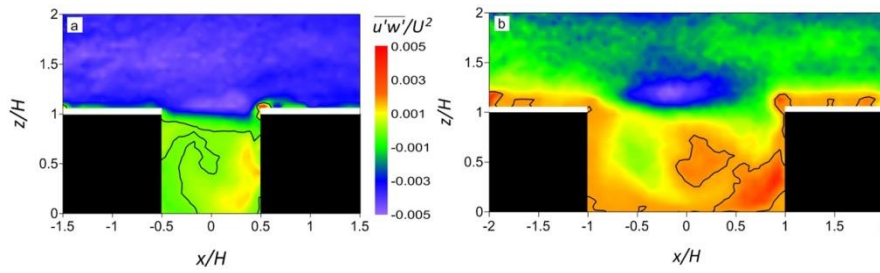


**Figure 3.** Non-dimensional vertical momentum flux  $(\overline{u'w'})/U^2$  maps for  $AR=1$  (a) and  $AR=2$  (b). The black line shows the passage from negative to positive values

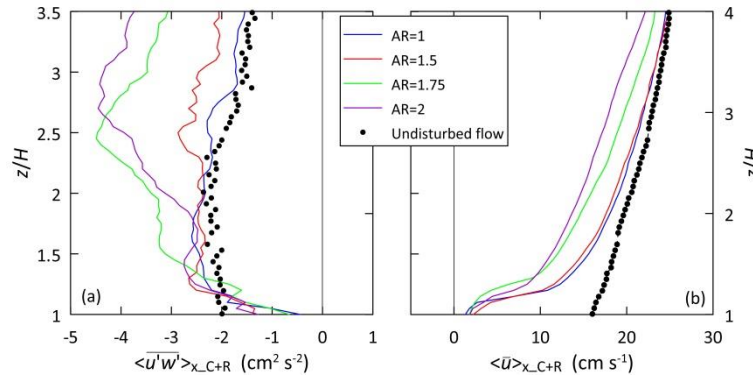


**Figure 4.** (a) Vertical profiles of the vertical momentum flux  $\langle \overline{u'w'}(z/H) \rangle_{x,C+R}$  averaged along the  $x$ -axis for different aspect ratios  $AR$ . (b) as in a), but for the streamwise velocity  $\langle \bar{u}(z/H) \rangle_{x,C+R}$

For  $AR=1$  and  $1.5$  (skimming flow) the maximum of  $\langle \overline{u'w'}(z/H) \rangle_{x,C+R}$  occurs at  $z/H \cong 1.25$ . Then, it remains nearly constant until  $z/H \cong 2.7$  and  $z/H \cong 3$  for  $AR=1$  and  $AR=1.5$ , respectively. Therefore,  $z/H \cong 1.25$  could be viewed as the upper boundary of the RSL, while a well-defined inertial sublayer (ISL) is present above, being the ISL the region above the RSL where the turbulent fluxes are nearly constant. Note that both  $\langle \overline{u'w'}(z/H) \rangle_{x,C+R}$  and  $\langle \bar{u}(z/H) \rangle_{x,C+R}$  for  $AR=1$  and  $AR=1.5$  share nearly the same profiles, suggesting that in cases of skimming flows those quantities are practically insensitive to the precise value of  $AR$ . In contrast, for  $AR=1.75$  and  $2$  (wake interference regime) the maximum of  $\langle \overline{u'w'}(z/H) \rangle_{x,C+R}$  occurs above  $z/H \cong 3$  and the constant flux layer does not seem to be present. The corresponding streamwise velocity profiles (Figure 4b) follow a log-law for  $z/H \gtrsim 1.7$  when  $AR=1$  and  $1.5$ , while the log-law does not hold for  $AR=1.75$  and  $2$ .

Given the lack of measurement along the y-axis, the quantity  $\text{TKE2D} = [\overline{u'^2} + \overline{w'^2}]/(2U^2)$  is used here as a proxy for the turbulent kinetic energy (TKE). Inside the canyon TKE2D maxima take place close to the windward building irrespective of AR (Figure 5), showing values twice those observed close to the leeward building wall. High levels of TKE2D occur also along the windward wall, according with Caton et al. (2003). The maximum value reached inside the canyon increases significantly with AR, as a result of the large region inside the canyon with large values of the variance of the vertical velocity component.

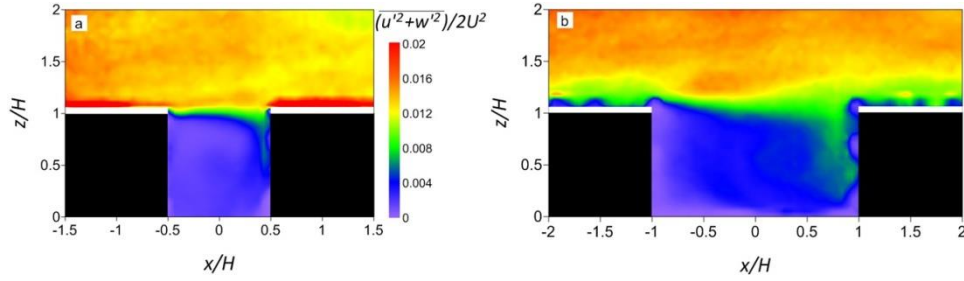


**Figure 5.**  $\text{TKE2D} = [\overline{u'^2} + \overline{w'^2}]/(2U^2)$  maps for (a) AR=1 and (b) AR=2

### Skewness

Knowledge of skewness factors can be useful, e.g. to dispersion modellers in that they are included in particle trajectory equations of Lagrangian stochastic models. As an example, maps of the skewness factor  $Sk_u = \overline{u'^3}/(\overline{u'^2})^{3/2}$  of the horizontal velocity component for AR=1 and 2 are reported in Figure 6a and 6b, respectively.  $Sk_u$  is negative almost everywhere inside the canyon for both ARs, except near the canyon top, where, for AR=1, a region of large, positive  $Sk_u$  is present. For AR=2, large (positive)  $Sk_u$  are located also near the buildings top.

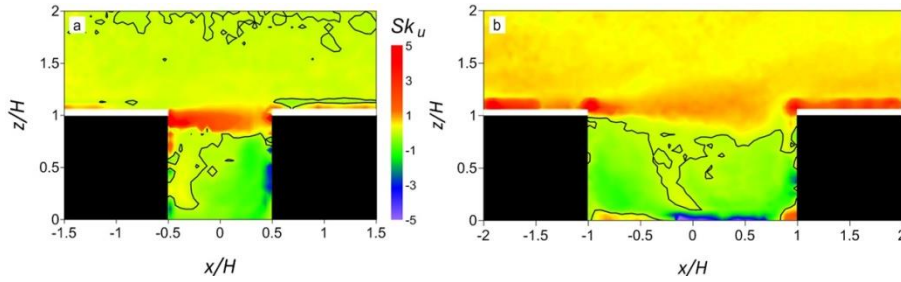


**Figure 6.** Horizontal velocity skewness factor  $Sk_u$  maps for (a) AR=1 and (b) AR=2. The black line identifies the transition from negative to positive values

### Shear production and dissipation rate of TKE

The shear production term,  $P = -\overline{u'_i u'_j} (\partial \overline{u}_i / \partial x_j)$ , and the rate of dissipation of TKE,  $\varepsilon$ , are presented in Figures 7 and 8, respectively (here,  $i=1,2,3$  and  $j=1,2,3$  indicate the axis of the coordinate system).  $\varepsilon$  was estimated starting from the two components of the fluctuating strain rate tensor (Hinze J., 1975), viz.:

$$\varepsilon = \frac{15}{4} \nu \left[ \left( \frac{\partial w'}{\partial z} \right)^2 + \left( \frac{\partial w'}{\partial z} \right)^2 \right] \quad (1)$$

The non-dimensional production term  $PH/U^3$  is positive above the canyon top, particularly for AR=1 (Figure 7a), where a well-defined region of maxima is present. That area corresponds with the mixing layer which develops after the trailing edge of the upstream obstacle and it is characterized by strong vertical shear. For AR=2 (Figure 7b) the region of  $PH/U^3$  maxima is still present, even though it is less evident with respect to AR=1. Those two regions are characterized by large vorticity (not shown) generated mainly at the canyons tops. Maxima of  $\varepsilon$  are located mainly above the canopy (Figure 8),

particularly close to the rooftops. Inside the canyon,  $\varepsilon$  roughly shows patterns similar to those observed for TKE, i.e. a region of maxima close to the windward building.

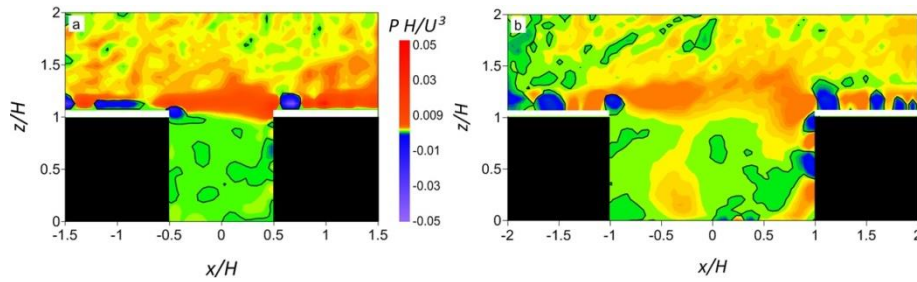


**Figure 7.**  $PH/U^3$  for (a)  $AR=1$  and (b)  $AR=2$ . The black line refers to the transition from negative to positive values.

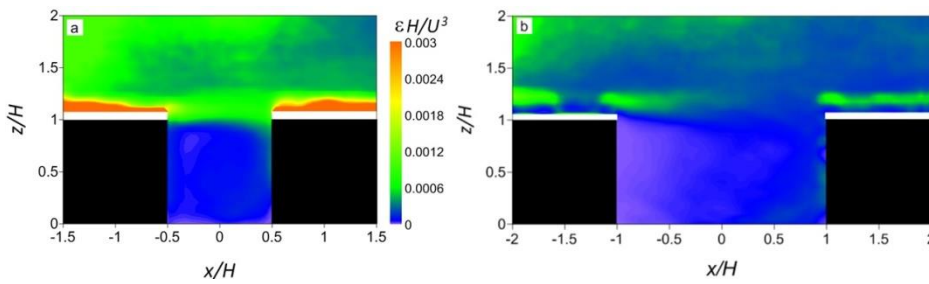


**Figure 8.** Maps of  $\varepsilon H/U^3$  and for (a)  $AR=1$  and (b)  $AR=2$ .

## CONCLUSIONS

The principal aim of this work was the experimental analysis of the turbulent flow which characterizes a 2D urban canopy layer. The study concerned two different flow regimes as a function of the aspect ratio  $AR$ : skimming flow ( $AR=1$ ) and wake interference regime ( $AR=2$ ). The results suggest that the proposed approach is a useful research tool for investigating canopy flows. Future work is in progress to analyse transport and dispersion of pollutants for the same canyon geometry.

## REFERENCES

- Caton F., R.E. Britter, S. Dalziel, 2003: Dispersion mechanisms in a street canyon. *Atmos. Environ.*, **37**, 693-702.
- Hinze J., 1975: Turbulence McGraw-Hill, New York.
- Jeong S. J. and M.J. Andrews, 2002: Application of the  $k-\varepsilon$  turbulence model to the high Reynolds number skimming flow field of an urban street canyon. *Atmos. Environ.*, **36**, 1137-1145.
- Kastner-Klein P., M.W. Rotach, 2004: Mean flow and turbulence characteristics in an urban roughness sublayer. *Boundary-Layer Meteorol.*, **111**, 55-84.
- Li X.-X., R.E. Britter, T.Y. Koh, L. K. Nordford, C.-H. Liu, D. Entekhabi, D.Y.C. Leung, 2010: Large-Eddy Simulation of Flow and Pollutant Transport in Urban Street Canyons with ground heating. *Boundary-Layer Meteorol.*, **137**, 187-204.
- Lien F. S., B. Yee, Y. Cheng, 2004: Simulation of mean flow and turbulence over a 2D building array using high-resolution CFD and a distributed drag force approach. *J. Wind. Eng. Ind. Aerodyn.*, **92**, 117-158.
- Miozzi M., B. Jacob, A. Olivieri, 2008: Performances Of Feature Tracking In Turbulent Boundary Layer Investigation. *Exp. Fluids*, **45**, 765-780.
- Oke T., 1987: Boundary-Layer Climates. Routledge, London.
- Pelliccioni A., P. Monti, G. Leuzzi, 2014: An alternative wind profile formulation for urban areas in neutral condition. *Environ. Fluid Mech.*, DOI: 10.1007/s10652-014.9364-1.
- Salizzoni P., M. Marro, L. Soulhac, N. Grosjean, R. J. Perkins, 2011: Turbulent transfer between street canyons and the overlying atmospheric boundary layer. *Boundary-Layer Meteorol.*, **141**, 393-414.
- Soulhac L., R. J. Perkins, P. Salizzoni, 2008: Flow in a street canyon for any external wind direction. *Boundary-Layer Meteorol.*, **126**, 365-388.